A Lattice Model for Computing the Transmissivity of the Cornea and Sclera

David B. Ameen, Marilyn F. Bishop, and Tom McMullen
Department of Physics, Virginia Commonwealth University, Richmond, Virginia 23284-2000 USA

ABSTRACT The method of photonic band structure is used to calculate the frequencies of light that propagate in lattice models of the cornea and sclera of the mammalian eye, providing an explanation for transparency in the cornea that first properly accounts for multiple scattering of light. Each eye tissue is modeled as an ordered array of collagen rods, and photonic band structure methods are used to solve Maxwell's equations exactly for these models, a procedure that automatically effectively includes all orders of multiple scattering. These calculations show that the dispersion relation for the cornea is linear in the visible range, implying that the cornea is transparent. We show that the transmissivity is ~97% by using an effective medium approximation derived from the photonic band structure results and applicable in the visible region. In contrast, the dispersion relation for the model in the sclera is not linear in the visible region, and there are band gaps in this region that could play an important role in the transmission of light in the sclera.

INTRODUCTION

The explanation for transparency in the cornea and opacity in the sclera of the mammalian eye has been sought and debated for many years (Maurice, 1957, 1969; Farrell and Hart, 1969; Hart and Farrell, 1969; Benedek, 1971; Vaezy and Clark, 1991). The qualitative explanation currently in the literature is that the average distance between the collagen fibrils that compose each of these tissues determines whether the tissues will be transparent or opaque (Benedek, 1971; Vaezy and Clark, 1991). The calculations behind this explanation do not account for all orders of multiple scattering of light, and these calculations for transparency versus opacity, which assume single scattering, can lead to a prediction of opacity in an ordered system that is actually transparent. Here we publish the results of a new approach (Ameen, 1996; Ameen et al., 1996) to the study of light propagation in the cornea and sclera. The approach employs photonic band structure (John, 1987; Yablonovitch, 1987), a method in which a determination is made of the frequencies of light that are allowed to propagate through a medium that consists of an ordered array of two components with different dielectric constants. In the present study, both the cornea and sclera are modeled as consisting of an ordered array of collagen rods embedded in a water-based background. The photonic band structure calculations solve Maxwell's equations exactly and so automatically effectively include all orders of multiple scattering in the propagation of light through the system.

Although the cornea is not perfectly ordered, and the sclera is highly disordered, the use of periodic models for which Maxwell's equations can be solved exactly gives a better idea of the basic physics of the system than considering scattering from a single fiber and trying to combine those single-particle scattering fields together to make up a solid. Our calculations can be considered to be first approximations to the system, and effects of disorder can be postponed until later as perturbations on the periodic systems. This is the approach used in solid-state physics in the study of the electronic structure of disordered systems. It is considered important to understand first the properties of the analogous periodic system before tackling the disordered one. Therefore, we have adopted that philosophy here. The problem of disorder in electronic structure continues to be an extremely challenging problem, and research is only beginning in the complicated photonic case of interest here.

One of the interesting effects that have been discovered by condensed-matter physicists studying photonic band structure is that some ordered physical systems have intervals of frequency in which electromagnetic waves cannot propagate. These forbidden frequency intervals are often called band gaps, in analogy with the band structure of electrons in periodic crystals. Actually, analogous photon stop bands have been known for many years in other contexts. For instance, photon stop-bands involved in the Restrahl region of ionic crystals were discovered in the 1920s. Here light couples to the optical vibrational modes of a crystal to produce photon-branch polaritons (see, for example, Born and Huang, 1968, especially Figs. 18 *a* and 19 *a–d*). A similar system involves the coupling of light to excitons to form exciton-polaritons (Hopfield, 1966). Both of these systems involve light coupling to an excitation of the system, whereas in the present case, light couples to a static periodic structure of the system.

Yablonovitch (1987) presented a discussion of how such a band gap could originate in photonic band structure, and at about the same time John developed the framework for photonic band structure calculations (John, 1987). The first calculation of a photonic band structure was made by John and Rangarajan (1988). This interest in photonic band gaps

Received for publication 23 April 1997 and in final form 31 July 1998.

Address reprint requests to Dr. Marilyn F. Bishop, Department of Physics, Virginia Commonwealth University, Box 842000, 1020 West Main St., Richmond, VA 23284-2000. Tel.: 804-828-1819; Fax: 804-828-7073; E-mail: bishop@gems.vcu.edu.

0006-3495/98/11/2520/12 $2.00

began with the desire to control the optical properties of materials to develop new types of optical devices. For instance, in fiber optic cables, if a cable turns a corner too sharply, the angle of incidence is too large for total internal reflection to occur, causing light to escape at the corners. This loss can be prevented by using a photonic crystal whose band gap is in the frequency range of the light being transported through the cable. This idea has wide applications not only in fiber optic networks, but also in devices that use optoelectronic circuits, in which light must be guided from one end of a microchip to another (Joannopoulos et al., 1995). Here we examine the photonic band structure (the band structure for photons) to investigate the transmission properties of light in ordered models of eye tissues to better understand the transparency of the cornea. This work is just the first step in understanding light propagation in eye tissues and was chosen because of its relative simplicity. We will also present an initial crude attempt at understanding why the sclera is not transparent, by seeing what happens in an ordered model with the sclera's physiological sizes and spacings of collagen.

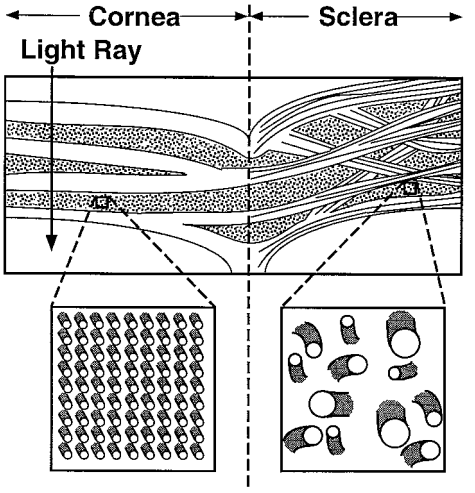

FIGURE 2 Structures of the cornea and the sclera. This figure is an enlargement of the portion of Fig. 1 enclosed by the rectangle. The collagen fibrils of the cornea are illustrated as perfectly ordered, as in the idealized lattice model to be used here, although electron micrographs show some disorder. The front of the eyeball, through which light enters, is at the top of the figure.

Physical systems

The physical systems examined in the present study include both the cornea, a thin transparent layer covering the lens of the eye, and the sclera, the white of the eye. These can be seen in Fig. 1, which is based on a figure from Kronfeld (1969). Together, these two tissues form the tough protective covering for the eyeball (Maurice, 1969). In addition, the curvature and transparency of the cornea enable it to provide 75% of the light refraction necessary for sight. Each of these eye tissues consists of collagen fibrils embedded in a water-based mucopolysaccharide background, and the fibrils and background substance have different dielectric constants. Even though both tissues have the same basic two-component composition, the respective fibril sizes and arrangements are different, as illustrated in Fig. 2, which is also based on a figure from Kronfeld (1969). In the cornea, the collagen fibrils are of relatively uniform diameter and spacing, and they are arranged as long parallel rods. These fibrils are grouped in sheets called lamellae that are parallel to the cornea's surface, so that the fibrils themselves are parallel to the cornea's surface. Whereas all of the fibrils in a given lamella are parallel to each other, the fibrils in adjacent lamellae need not be. In the sclera, the fibrils have larger diameters and spacing than in the cornea, and their diameters, spacing, and orientation vary randomly.

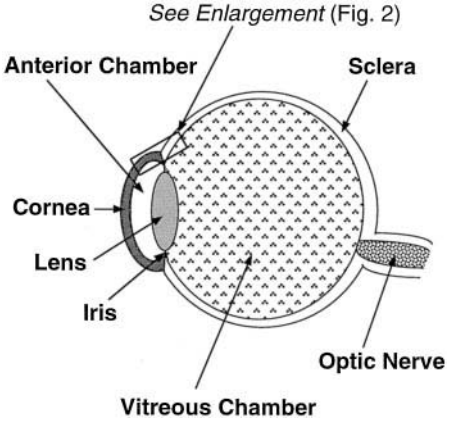

FIGURE 1 Horizontal cross section of the right eye viewed from above. The eyeball is covered by the cornea and the sclera. The rectangle enclosing a region where the cornea joins the sclera is enlarged in Fig. 2.

History

It has been asked why the cornea is transparent whereas the sclera is opaque, even though the volume fractions of collagen and background are essentially the same. If one were to consider the cornea to have a homogeneous composition with a uniform real index of refraction, it would be transparent, because all frequencies of light could propagate through it. Maurice pointed out that the cornea actually consists of two components, as found by electron microscopy, which have different indices of refraction, and searched for an alternative explanation for the transparency (Maurice, 1957). He began by using the fraction of light scattered by an isolated cylinder with the appropriate indices of refraction for the collagen and background. He showed that if one adds the intensities of light scattered from each fibril, then 94% of the light would be scattered, suggesting that the cornea would be opaque. To resolve this paradox, he suggested that if the actual arrangement of the fibrils were completely ordered as in a crystal lattice, interference effects might allow transparency. Indeed, electron micrographs showed some degree of order.

In subsequent studies, Hart and Farrell and Benedek attempted to determine whether ordering in the cornea could produce the desired interference effects (Hart and Farrell, 1969; Benedek, 1971). These authors, however, disagreed with Maurice's hypothesis that the fibrils must be in a completely ordered array for transparency to be permitted. Instead they proposed that even the partial order in fibril arrangement found in electron micrographs would create enough cancellation of scattered intensity to allow transparency. An essential difference in their calculation, when compared to that of Maurice, was that they summed the electric fields before squaring them to obtain the intensities. This procedure of summing the amplitudes before squaring to find the intensities gives some cancellation, which these authors called the interference effects. These fields were summed by using the pair correlation functions of the positions of the fibrils as obtained from electron micrograph studies. Hart and Farrell's calculation gave over 80% of the light to be transmitted by the cornea. Hart and Farrell also showed that using the pair correlation function for fibrils in totally uncorrelated positions is equivalent to Maurice's estimate of summed intensities in place of amplitudes and found, after correcting an error by Maurice, that 92% of the light was scattered and only 8% transmitted in that approximation. Their calculation agreed with experimental data for long wavelengths (7000–8000 Å) but had a peculiar wavelength dependence at shorter wavelengths not present in the experimental data. The calculation did not include absorption effects, because of the extreme difficulty of such calculations, although these effects could have been a factor in the wavelength dependence of the experiments.

Hart and Farrell's and Benedek's work, like that of Maurice, used electric fields describing light that is scattered only by an isolated fibril. Benedek suggested that whenever the spacing of the fibrils is significantly smaller than the wavelength of visible light, the amount of scattering must be small and the tissue transparent (Benedek, 1971). He also suggested that the medium would be opaque if the spacing were of the order of the wavelength of visible light or larger, as in the sclera. Inspired by this proposal, Vaezy and Clark used scanning transmission electron microscopy to measure the spectral density of the two-dimensional density fluctuations in the cornea and sclera. They supposed that the refractive index of the material scaled with the density and, consequently, that this measurement gave the spatial *Fourier* components of the refractive index fluctuations. They interpreted their results as confirming the proposal that the transparency and opacity of structures of the eye are determined by the size and spacing of the collagen fibrils in the tissue (Vaezy and Clark, 1991).

Inclusion of multiple scattering

In dense systems like eye tissues, light bounces many times off many fibrils. This is called multiple scattering. This must not be confused with classical particle scattering, because the situation for waves is more complex because of wave interference. For light waves, the amplitude has to be summed over all possible paths through the collection of fibrils before squaring to find the intensity. This is why a classical diffusion approximation does not work for light, and why the approximation of attenuating the incident beam analogous to using Beer's law also misses the interference effects that arise from multiple scattering. To study the transmission of light through the system, which is generally disordered, one should ideally solve Maxwell's equations exactly, but only limited progress has been made toward this goal. For disordered systems, some progress has been made on the question of localization of light, where destructive interference prevents photons from propagating (John, 1993). However, in the limiting case of a perfectly periodic system, Maxwell's equations can be solved exactly. The methods for doing this were developed in solid-state physics and are called photonic band structure calculations (Yablonovitch, 1987; John and Rangarajan, 1988; Economou and Zdetsis, 1989; Yablonovitch and Gmitter, 1989; Ho et al., 1990; Leung and Liu, 1990a,b; Zhang and Satpathy, 1990; Plihal and Maradudin, 1991; Maradudin and McGurn, 1993; Cassagne et al., 1995; Joannopoulos et al., 1995). To apply this method, we approximate the fibril arrangement in the cornea by a periodic array, and indeed the fibrils in the cornea do exhibit a substantial degree of order (Vaezy and Clark, 1991). Although the sclera has a considerable degree of disorder in the distribution of its fibrils (Vaezy and Clark, 1991), we also use an ordered model for this system. This will allow us to determine whether the distance between fibrils in the cornea and sclera is such that light propagates through the system as if it were a uniform medium, or whether the structure of the rods has an effect on the propagation of light. Our ordered model for the sclera has a spacing equal to the average spacing in the actual sclera, which is on the order of the wavelength of visible light. The single-scattering spacing hypothesis predicts that our ordered model of the sclera would be opaque. Although we will not be able to solve the model that includes the effects of disorder to comment conclusively on the opacity of the sclera, our calculations will be the first step in understanding the role of the spacing of the rods in a calculation that has effectively included multiple scattering effects to all orders.

PHOTONIC BAND STRUCTURE

Light propagation in homogeneous media

To characterize the propagation of electromagnetic radiation through the cornea and sclera, we will use photonic band structure theory to solve Maxwell's equations. We will assume that there are no free charges, no free currents, and zero magnetic susceptibility. Before we introduce photonic band structure theory, it is instructive to begin with a medium that is uniform and isotropic. The derivation starts

with Fourier-transforming Maxwell's equations (Reitz et al., 1993) in time to obtain (in cgs units)

$$\nabla \cdot \vec{D} = 0 \quad \nabla \times \vec{E} = \frac{i\omega}{c}\vec{B}$$
$$\nabla \cdot \vec{B} = 0 \quad \nabla \times \vec{H} = -\frac{i\omega}{c}\vec{D}, \tag{1}$$

with the constitutive relations for a nonmagnetic medium,

$$\vec{D} = \epsilon\vec{E}; \quad \vec{B} = \vec{H}. \tag{2}$$

When the dielectric constant ϵ, which is equivalent to the square of the refractive index, is independent of the spatial variables, eliminating $\vec{D}$ and $\vec{B}$ leads to the differential equations

$$\nabla^2\vec{E} + \frac{\epsilon\omega^2}{c^2}\vec{E} = 0 \tag{3}$$

$$\nabla^2\vec{H} + \frac{\epsilon\omega^2}{c^2}\vec{H} = 0, \tag{4}$$

where $\vec{E}$ and $\vec{H}$ are the electric and magnetic field vectors and c is the speed of light in a vacuum. These equations have the form of eigenvalue equations in which ω^2 is the eigenvalue. The eigenfunctions are

$$\vec{E}(\vec{r}, \omega) = \vec{E}_0 e^{i\vec{k}\cdot\vec{r}} \tag{5}$$

and

$$\vec{H}(\vec{r}, \omega) = \vec{H}_0 e^{i\vec{k}\cdot\vec{r}}, \tag{6}$$

in which $\vec{E}_0$ and $\vec{H}_0$ are constants, $\vec{k}$ is the wave vector, $\vec{r}$ is the position in three-dimensional space, and where the angular frequency ω is related to $\vec{k}$ by

$$\omega(k) = \frac{c}{\sqrt{\epsilon}}k. \tag{7}$$

Dielectric lattice models

In the cornea and sclera, the differing dielectric constants of the collagen fibrils and the background substance cause light to propagate in a more complicated manner than the simple plane waves of Eqs. 5 and 6. We model the cornea and sclera by periodic arrays of infinitely long cylindrical collagen fibrils parallel to the z axis, as shown in Fig. 3. These fibrils have a dielectric constant ϵ_f and are embedded in a mucopolysaccharide background material of dielectric constant ϵ_b. Because the collagen fibrils lie parallel to the outer surfaces of the cornea and sclera, the light that is at normal incidence on these surfaces is perpendicular to the rod axes, with the direction of light propagation in the xy plane. We consider two polarizations of light. The first, called $\vec{E}_\perp$ polarization, has the electric field perpendicular to the fibrils and consequently in the xy plane. The second, called $\vec{E}_\parallel$ polarization, has the electric field vector parallel to the axes of the fibrils and in the z direction. These choices are convenient because these two polarizations propagate independently of one another in this geometry.

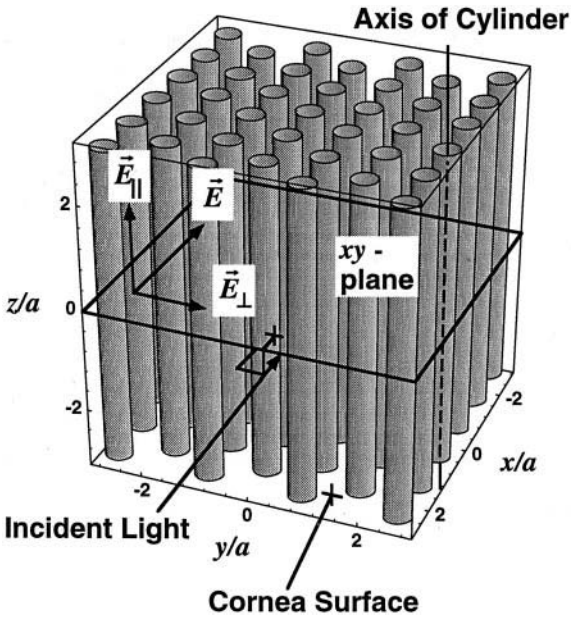

FIGURE 3 The cornea modeled as an ordered array of collagen fibrils. The fibrils are idealized as parallel cylindrical rods. These rods are parallel to the cornea surface and so are perpendicular to the plane in which the light propagates, denoted the xy plane here. The lattice constant a is the distance separating the central axes of adjacent rods. The electric field $\vec{E}$ of the light passing through the tissue lies in the plane of the cornea surface and is conveniently resolved into components that are parallel and perpendicular to the rods.

The particular periodic array that we choose is the close-packed arrangement in which the fibril centers lie on the two-dimensional triangular lattice shown in Fig. 4. This model for the cornea and sclera involves the same lattice structure as the semiconductor dielectric lattice model described by Plihal and Maradudin (1991), and we use an approach similar to theirs to calculate the photonic bands. Positions are projected onto the xy plane as

$$\vec{r}_\parallel = \hat{x}x + \hat{y}y, \tag{8}$$

so that the vector $\vec{r}_\parallel$ lies in the xy plane. The lattice positions are integer multiples of the primitive lattice translation vectors given by

$$\vec{a}_1 = a(1, 0) \tag{9}$$

$$\vec{a}_2 = a\left(\frac{1}{2}, \frac{\sqrt{3}}{2}\right), \tag{10}$$

where a is the distance between the centers of adjacent fibrils, and the area of the primitive unit cell is

$$a_c = |\vec{a}_1 \times \vec{a}_2| = \frac{\sqrt{3}}{2}a^2. \tag{11}$$

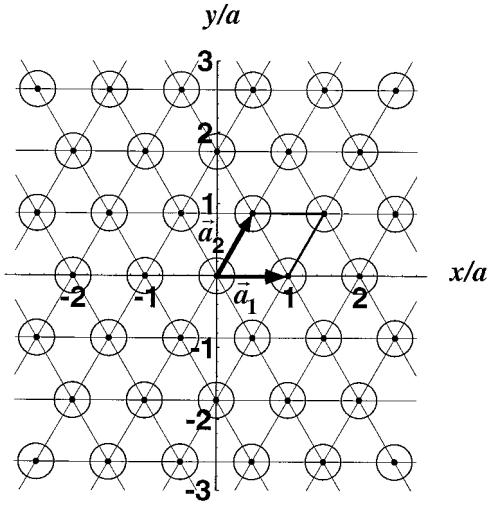

FIGURE 4 A two-dimensional triangular lattice. This lattice is used to model the array of collagen fibrils, with each fibril represented as a cylindrical rod perpendicular to the *xy* plane, which is the plane in which light propagates through the cornea. The lengths of both primitive lattice vectors $\vec{a}_1$ and $\vec{a}_2$ are the lattice constant a. The primitive unit cells are parallelograms with sides given by the primitive lattice vectors, and one of these primitive unit cells is highlighted.

Photonic band structure formalism

For the dielectric lattice, Maxwell's equations must be solved for a dielectric constant $\epsilon(\vec{r}_\parallel)$ that depends on position, because the dielectric constant inside the fibril is different from its value in the background material. In a periodic lattice of fibrils, $\epsilon(\vec{r}_\parallel)$ is a periodic function, and so these equations can be solved using photonic band structure methods, as we will describe below. (Maradudin and McGurn, 1993). For the $E_\perp$ polarization the electric field is perpendicular to the long axes of the collagen rods, and a solution is sought that has the form

$$\vec{E}_\perp(\vec{r}_\parallel, \omega) = \hat{x}E_x(\vec{r}_\parallel, \omega) + \hat{y}E_y(\vec{r}_\parallel, \omega) \tag{12}$$

$$\vec{H}_\perp(\vec{r}_\parallel, \omega) = \hat{z}H_z(\vec{r}_\parallel, \omega). \tag{13}$$

For the $E_\parallel$ polarization the electric field is parallel to the long axes of the collagen rods, and a solution is sought that has the form

$$\vec{E}_\parallel(\vec{r}_\parallel, \omega) = \hat{z}E_z(\vec{r}_\parallel, \omega) \tag{14}$$

$$\vec{H}_\parallel(\vec{r}_\parallel, \omega) = \hat{x}H_x(\vec{r}_\parallel, \omega) + \hat{y}H_y(\vec{r}_\parallel, \omega). \tag{15}$$

Substituting these into Maxwell's equations leads to a partial differential equation in a single field component for each polarization of the electric field. For $E_\perp$ polarization, it is simplest to use the $\vec{H}$ equation (Eq. 4), which is an equation for H_z alone. The only difference from Eq. 4 is that a derivative of $\epsilon(\vec{r}_\parallel)$ now appears, because the dielectric function now has a spatial dependence. This gives

$$\frac{\partial}{\partial x}\left[\frac{1}{\epsilon(\vec{r}_\parallel)}\frac{\partial H_z(\vec{r}_\parallel, \omega)}{\partial x}\right] + \frac{\partial}{\partial y}\left[\frac{1}{\epsilon(\vec{r}_\parallel)}\frac{\partial H_z(\vec{r}_\parallel, \omega)}{\partial y}\right] + \frac{\omega^2}{c^2}H_z(\vec{r}_\parallel, \omega) = 0. \tag{16}$$

Similarly, for the $E_\parallel$ polarization, it is simplest to use the $\vec{E}$ equation (Eq. 3), which is an equation for E_z alone. This gives

$$\frac{1}{\epsilon(\vec{r}_\parallel)}\left(\frac{\partial^2}{\partial x^2} + \frac{\partial^2}{\partial y^2}\right)E_z(\vec{r}_\parallel, \omega) + \frac{\omega^2}{c^2}E_z(\vec{r}_\parallel, \omega) = 0. \tag{17}$$

Because $\epsilon(\vec{r}_\parallel)$ is periodic with the periodicity of the lattice, Bloch's Theorem allows us to write the solution to these equations (Eqs. 16 and 17) as the product of a plane wave with wave vector $\vec{k}_\parallel$ and a function that has the periodicity of the lattice, as we will see.

To take advantage of the periodicity of the lattice in solving Eqs. 16 and 17, it is useful to define the two-dimensional reciprocal lattice corresponding to the triangular array of Fig. 4. The sites of this reciprocal lattice are found by translating a single primitive unit cell by various reciprocal lattice vectors, which are integral multiples of the primitive translation vectors of the reciprocal lattice $\vec{b}_1$ and $\vec{b}_2$, defined by

$$\vec{a}_i \cdot \vec{b}_j = 2\pi\delta_{ij} \quad i, j = 1, 2. \tag{18}$$

For the triangular lattice, using Eqs. 9 and 10, these primitive translation vectors are given explicitly by

$$\vec{b}_1 = \frac{2\pi}{a}\left(1, -\frac{\sqrt{3}}{3}\right) \tag{19}$$

$$\vec{b}_2 = \frac{2\pi}{a}\left(0, \frac{2\sqrt{3}}{3}\right). \tag{20}$$

Then the reciprocal lattice vectors can be written as

$$\vec{G}_\parallel = n_1\vec{b}_1 + n_2\vec{b}_2, \tag{21}$$

with n_1 and n_2 integers.

We need these reciprocal lattice vectors because if one expands a periodic function in a Fourier series, only these wave vectors appear in that expansion. Bloch's Theorem states that the solution to Eq. 16 can be written in the form

$$H_z(\vec{r}_\parallel) = u_{\vec{k}_\parallel}(\vec{r}_\parallel)e^{i\vec{k}_\parallel \cdot \vec{r}_\parallel}, \tag{22}$$

where $u_{\vec{k}_\parallel}(\vec{r}_\parallel)$ is a function with the periodicity of the lattice. The solution for $E_z(\vec{r}_\parallel)$ is analogous to that in Eq. 22.

When the periodic function $u_{\vec{k}_\parallel}(\vec{r}_\parallel)$ is expanded in plane waves, the only wave vectors that appear are those corresponding to the reciprocal lattice vectors $\vec{G}_\parallel$, so that

$$H_z(\vec{r}_\parallel, \omega) = \left[\sum_{\vec{G}_\parallel} A_{\vec{k}_\parallel}(\vec{G}_\parallel)e^{i\vec{G}_\parallel \cdot \vec{r}_\parallel}\right]e^{i\vec{k}_\parallel \cdot \vec{r}_\parallel} \tag{23}$$

and

$$E_z(\vec{r}_\parallel, \omega) = \left[\sum_{\vec{G}_\parallel} \frac{A_{\vec{k}_\parallel(\vec{G}_\parallel)}}{|\vec{k}_\parallel + \vec{G}_\parallel|} e^{i\vec{G}_\parallel \cdot \vec{r}_\parallel}\right] e^{i\vec{k}_\parallel \cdot \vec{r}_\parallel}. \tag{24}$$

In Eq. 24, the factor of $|\vec{k}_\parallel + \vec{G}_\parallel|$ in the denominator appears to make future equations simpler and merely redefines the unknown coefficients $A_{\vec{k}_\parallel}(\vec{G}_\parallel)$. These are actually Fourier series expansions of the fields in which, because of the periodicity of the lattice, only the Fourier coefficients that differ by reciprocal lattice vectors appear. To solve for the relation between frequency and wave vector that allows solutions to Eqs. 16 and 17, it is necessary to write the functional form of the reciprocal dielectric constant $1/\epsilon(\vec{r}_\parallel)$. This can be represented in terms of the step function $\Theta(\vec{r}_\parallel)$, such that

$$\Theta(\vec{r}_\parallel) = \begin{cases} 1, & \vec{r}_\parallel \quad \text{inside fibrils} \\ 0, & \vec{r}_\parallel \quad \text{outside fibrils.} \end{cases} \tag{25}$$

Then the reciprocal dielectric function $1/\epsilon(\vec{r}_\parallel)$ becomes

$$\frac{1}{\epsilon(\vec{r}_\parallel)} = \frac{1}{\epsilon_b} + \left(\frac{1}{\epsilon_f} - \frac{1}{\epsilon_b}\right)\Theta(\vec{r}_\parallel). \tag{26}$$

Because $1/\epsilon(\vec{r}_\parallel)$ has the periodicity of the lattice, it can also be expanded in plane waves by using the reciprocal lattice vectors:

$$\frac{1}{\epsilon(\vec{r}_\parallel)} = \sum_{\vec{G}_\parallel} \kappa(\vec{G}_\parallel) \exp(i\vec{G}_\parallel \cdot \vec{r}_\parallel), \tag{27}$$

where

$$\kappa(\vec{G}_\parallel) = \begin{cases} \dfrac{1}{\epsilon_f} f + \dfrac{1}{\epsilon_b}(1-f), & \vec{G}_\parallel = 0, \\ f\left(\dfrac{1}{\epsilon_f} - \dfrac{1}{\epsilon_b}\right)\left(\dfrac{2J_1(G_\parallel R)}{G_\parallel R}\right), & \vec{G}_\parallel \neq 0, \end{cases} \tag{28}$$

where $J_1(G_\parallel R)$ is a Bessel function of order one and f is the filling fraction, which is the ratio of the collagen fibril cross-sectional area to the unit cell area a_c given in Eq. 11.

Using this explicit form of the reciprocal dielectric function, the eigenvalue equations (Eqs. 16 and 17) become

$$\sum_{\vec{G}_\parallel'} [(\vec{k}_\parallel + \vec{G}_\parallel) \cdot (\vec{k}_\parallel + \vec{G}_\parallel')] \kappa(\vec{G}_\parallel - \vec{G}_\parallel') A_{\vec{k}_\parallel}(\vec{G}_\parallel') = \frac{\omega^2}{c^2} A_{\vec{k}_\parallel}(\vec{G}_\parallel) \tag{29}$$

for the $E_\perp$ polarization and

$$\sum_{\vec{G}_\parallel'} [|\vec{k}_\parallel + \vec{G}_\parallel||\vec{k}_\parallel + \vec{G}_\parallel'|] \kappa(\vec{G}_\parallel - \vec{G}_\parallel') A_{\vec{k}_\parallel}(\vec{G}_\parallel') = \frac{\omega^2}{c^2} A_{\vec{k}_\parallel}(\vec{G}_\parallel) \tag{30}$$

for the $E_\parallel$ polarization. These are both matrix eigenvalue equations of the form $M^\mu A = (\omega^2/c^2)A$, where

$$M_{ij}^{\perp} = [(\vec{k}_\parallel + \vec{G}_{\parallel,i}) \cdot (\vec{k}_\parallel + \vec{G}_{\parallel,j})] \kappa(\vec{G}_{\parallel,i} - \vec{G}_{\parallel,j}) \tag{31}$$

for $E_\perp$ polarization and

$$M_{ij}^{\parallel} = [|\vec{k}_\parallel + \vec{G}_{\parallel,i}||\vec{k}_\parallel + \vec{G}_{\parallel,j}|] \kappa(\vec{G}_{\parallel,i} - \vec{G}_{\parallel,j}) \tag{32}$$

for $E_\parallel$ polarization. For each polarization, the matrix M^μ defined in this way is symmetrical. The matrix equations for the $E_\perp$ and $E_\parallel$ polarizations, respectively, can be written explicitly in the form

$$\begin{bmatrix} M_{11} & M_{12} & M_{13} & \cdots \\ M_{21} & M_{22} & M_{23} & \cdots \\ M_{31} & M_{32} & M_{33} & \cdots \\ \vdots & \vdots & \vdots & \end{bmatrix} \begin{bmatrix} A_{\vec{k}_\parallel}(\vec{G}_{\parallel,1}) \\ A_{\vec{k}_\parallel}(\vec{G}_{\parallel,2}) \\ A_{\vec{k}_\parallel}(\vec{G}_{\parallel,3}) \\ \vdots \end{bmatrix} = \frac{\omega^2}{c^2} \begin{bmatrix} A_{\vec{k}_\parallel}(\vec{G}_{\parallel,1}) \\ A_{\vec{k}_\parallel}(\vec{G}_{\parallel,2}) \\ A_{\vec{k}_\parallel}(\vec{G}_{\parallel,3}) \\ \vdots \end{bmatrix}. \tag{33}$$

The unknown eigenvalues are ω^2/c^2, and the components of the unknown eigenvectors are $A_{\vec{k}_\parallel}(\vec{G}_{\parallel,j})$, which are the expansion coefficients for the space-dependent factors of the fields, as given in Eqs. 23 and 24. Diagonalization of the matrix for each polarization generates a set of frequencies for each wave vector $\vec{k}_\parallel$, leading to a set of photonic bands whose number equals the rank of the matrix, and each solution is labeled with a band index. In principle, this is a matrix of infinite rank, and its solution represents an exact solution to the problem. For numerical calculations, a matrix of finite rank must be used, and the accuracy of the solution increases with the rank of the matrix.

To choose a range of values of $\vec{k}_\parallel$ to use in Eqs. 31 and 32, we need to introduce the first Brillouin zone, which is the hexagon shown in Fig. 5, whose sides are perpendicular bisectors of the shortest reciprocal lattice vectors or, in other words, bisectors of the shortest lines between reciprocal lattice points, shown as the large dots. As is well known,

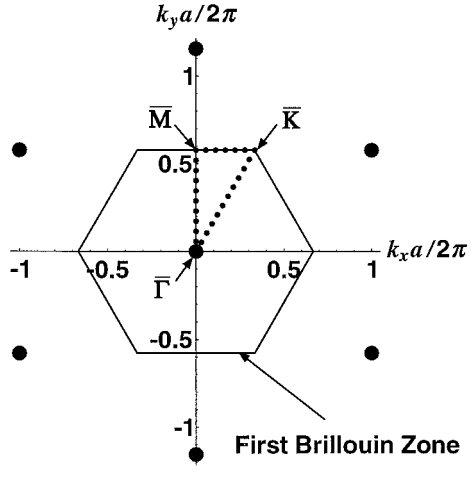

FIGURE 5 The two-dimensional reciprocal lattice corresponding to the triangular lattice of Fig. 4. The large dots show the reciprocal lattice points that correspond to the end points of the shortest reciprocal lattice vectors $\vec{G}_\parallel$. The first Brillouin zone is the hexagon shown and is formed by the perpendicular bisectors of the shortest reciprocal lattice vectors. The small dots outline the triangular path around the irreducible segment of the first Brillouin zone that we use to illustrate the photonic band structure in subsequent figures. The symbols are conventional labels for points in the Brillouin zone.

this scheme is useful because all solutions can be labeled, in addition to the band index, by a wave vector equivalent to $\vec{k}_{\|}$ that lies within the first Brillouin zone (see, for example Brillouin, 1953). If $\vec{k}_{\|}$ is chosen outside this zone, it is possible to find a reciprocal lattice vector $\vec{G}_{\|}$ such that $\vec{k}_{\|} + \vec{G}_{\|}$ lies inside this first Brillouin zone, and it can be shown that the form of the solution in Eq. 22 is unchanged. Because of symmetry, it is sufficient to consider only the irreducible one-twelfth of the zone outlined by the black dots in Fig. 5. As is standard in electronic band structure, the special points in the zone are labeled with the symbols $\bar{\Gamma}$, $\bar{M}$, and $\bar{K}$, as shown.

Calculations for the cornea lattice model

In this section, we describe our photonic band structure calculations for our periodic cornea model using the same parameters as Maurice (1957), with values for collagen radius and spacing chosen to be those of rabbit corneas, and the dielectric constants chosen to be those of oxen corneas. For the cornea, we use a fibril radius of $R = 15.5$ nm. For the lattice constant a, we use the average center-to-center distance of the collagen fibrils $a = 62$ nm. For these structural constants, the filling fraction, the fraction occupied by the fibrils, is given by $f = 0.23$. The values for the two dielectric constants are found by squaring the respective indices of refraction, giving $\epsilon_f = 2.40$ for collagen and $\epsilon_b = 1.809$ for the mucopolysaccharide background. Fig. 6 shows a plot of the lowest 10 eigenvalues ω versus $\vec{k}_{\|}$ obtained by diagonalizing the matrices given in Eq. 33, as $\vec{k}_{\|}$ traces out the dotted triangle in Fig. 5 from $\bar{\Gamma}$ to $\bar{M}$ to $\bar{K}$ and back to $\bar{\Gamma}$. Each dot in that triangle, or each corresponding point on the axis in Fig. 6, represents a vector $\vec{k}_{\|}$ drawn from the origin of the Brillouin zone to that dot. Each continuous curve in this figure is called a band. In this figure, frequencies are expressed in terms of the photon energy $\hbar\omega$, given in electron volts, and the corresponding vacuum wavelengths $\lambda = \omega/2\pi c$ are shown on the right axis. Visible light, which has vacuum wavelengths in the range of 400–700 nm, corresponds to frequencies that lie near the bottom of the lowest band, as shown. In this visible region, the lowest band has a nearly linear dispersion relation. In fact, because we have chosen the dielectric constants to be the values appropriate for the visible region, the calculations are not strictly meaningful outside this region if the dielectric constant is strongly frequency dependent. These bands do not include, for instance, the dispersion associated with electronic excitations that occurs in the ultraviolet, such as in the range of 190–250 nm (6.5–5.0 eV) (Feng et al., 1997), or the dispersion of the infrared spectra in the range of 3800–1200 cm^{-1} (2600–8300 nm or 0.5–0.1 eV) (Doyle et al., 1975).

These calculations were done at each of 50 evenly spaced points along the triangular path in the first Brillouin zone shown in Fig. 5. To establish convergence, 15 different matrix sizes were used, ranging from 7×7 to 755×755.

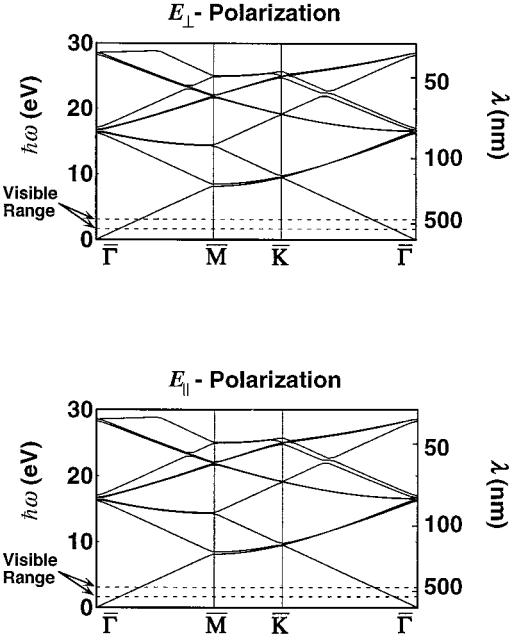

FIGURE 6 The first 10 photonic energy bands for the lattice model of the cornea. The horizontal axis represents the unfolded triangular path around the irreducible segment of the Brillouin zone shown in Fig. 5. As explained in the text, each point on that axis represents a wave vector $\vec{k}_{\|}$ drawn from the origin to the given point in the two-dimensional Brillouin zone. The photon energy $\hbar\omega$ is given in electron volts on the left axis and converted to vacuum wavelengths $\lambda = \omega/2\pi c$ on the right axis. Band structures for the two polarizations, light with the electric vector perpendicular to the fibrils (*upper*) and parallel to the fibrils (*lower*) are shown.

The numbers of reciprocal lattice vectors $\vec{G}_{\|}$ that formed these matrices were chosen to ensure that all of the reciprocal lattice vectors up to a given length were included. This is analogous to choosing both positive and negative frequencies up to a given cutoff frequency in a Fourier series. With each successively larger matrix, the frequencies converge closer to limiting values, with convergence being faster for the lower bands. Results presented in Fig. 6 are for the 755×755 matrix, although a 19×19 matrix was sufficient to give quite good convergence for the first 10 bands.

Calculations for the sclera lattice model

The sclera is also modeled as consisting of parallel collagen fibrils of uniform diameter and spacing so that a planar slice perpendicular to the long axes of the fibrils creates a triangular lattice. Although the actual sclera exhibits very little uniformity in the size and spacing of its collagen fibrils, the intention is to use a model that to first approximation has the same structure as the densely packed collagen in the sclera. In this way we will be able to determine what effect the average lattice spacing would have on the propagation of light in a periodic sclera-like material. That is, before embarking on a study of disorder in the sclera, for which calculations must necessarily be approximate, it is interest-

ing to know for the sclera fibril spacing the results of an exact calculation to understand clearly the effects of multiple scattering in such a material. In the future, the much more formidable task of approaching the disordered case could be considered. The fibril and background dielectric constants are identical to the values used in the cornea lattice model. To calculate the filling fraction, averages for the collagen fibril radius of $R = 60$ nm and spacing of $a = 250$ nm are determined from data presented by Vaezy and Clark (1991) for human sclera. The corresponding filling fraction, or the fractional volume occupied by collagen fibrils, is $f = 0.21$. The band structure found using these parameters is shown in Fig. 7. The upper part of the lowest band and the lower parts of the second and third bands lie in the visible range. This visible region includes band gaps at the Brillouin zone boundaries (points $\bar{M}$ and $\bar{K}$) between the lowest and the next two bands. Here, instead of the nearly linear dispersion relation found in the cornea, the bands bend over and become flat at the zone boundaries. The $\vec{k}_{\|}$ values at which the frequencies were calculated were chosen as in the previous section for the cornea, and similar convergence tests were done. Again, a 19×19 matrix gave quite good convergence for the first 10 bands, although Fig. 7 was constructed using results calculated with 755×755 matrices.

The empty lattice

The physics underlying the plots of photonic band structures like those shown in Figs. 6 and 7 is most easily understood by considering the example of what is called the empty lattice. Imagine an array of lattice sites located where the fibril centers would be in the cornea lattice model, but where these cylinders have exactly the same dielectric constant $\epsilon = \epsilon_b$ as that of the background medium. This is, of course, simply a uniform medium with the background dielectric constant, and the dispersion relation for the photons is simply the linear relation given by Eq. 7. However, consider what happens when this is plotted in the same way as the bands of Figs. 6 and 7. The linear dispersion relation in two dimensions is actually a cone. Suppose one places this cone with its apex at the origin of the picture of the Brillouin zone in Fig. 5. If the cone is now cut along the line from $\bar{\Gamma}$ to $\bar{M}$, for example, its edge traces out the lowest band from $\bar{\Gamma}$ to $\bar{M}$ shown in Fig. 8. One then draws higher Brillouin zones by bisecting lines to more distant reciprocal lattice points. Now one cuts the cones alone the lines in these higher Brillouin zones that correspond to the line from $\bar{\Gamma}$ to $\bar{M}$ in the first Brillouin zone. Those cut edges form the higher bands shown along $\bar{\Gamma}$ to $\bar{M}$ in Fig. 8. Similar construction along the lines from $\bar{M}$ to $\bar{K}$ and from $\bar{K}$ back to $\bar{\Gamma}$ gives the remaining portions of the bands in Fig. 8. Thus the plot of Fig. 8 is simply an unusual way (except in condensed-matter physics) of drawing a linear dispersion relation (Eq. 7) in two dimensions that is really just a cone (Ameen, 1996).

The photonic band structure shown in Fig. 6 for the cornea lattice model is similar to that for the empty lattice model. However, introduction of the physical lattice makes several changes in the band structure, as can be seen by comparing Figs. 6 and 8. One change is that the bands are often flat at the Brillouin zone boundaries and at the zone center $\bar{\Gamma}$ in all bands but the lowest. Others are that the degeneracies of bands are split and gaps are opened at the Brillouin zone boundaries. The twofold degeneracy of the lowest band from $\bar{M}$ to $\bar{K}$ in Fig. 8 splits visibly in Fig. 6. An example of a gap opening at the zone boundary can be seen at the $\bar{M}$ point for the lowest two bands in Fig. 6.

The splittings in Fig. 6 are fairly small because the dielectric contrast, although typical of biological materials,

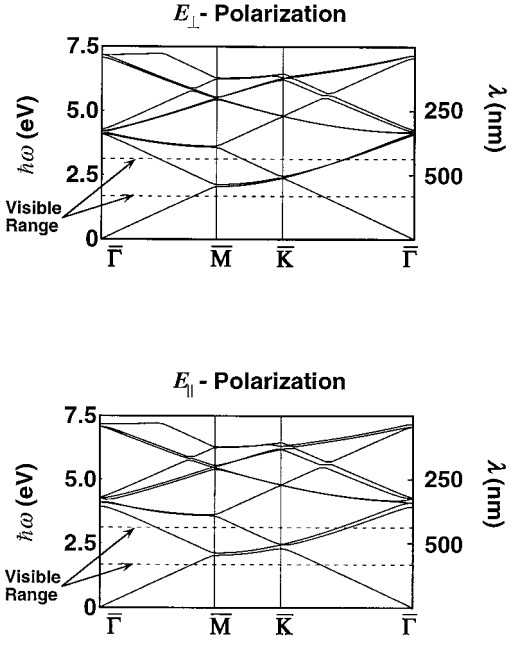

FIGURE 7 The first 10 photonic energy bands for the lattice model of the sclera. The horizontal axis represents the triangular path around the irreducible segment of the Brillouin zone (Fig. 5), as in Fig. 6. The photon energy $\hbar\omega$ is given in electron volts and as the corresponding vacuum wavelength $\lambda = \omega/2\pi c$.

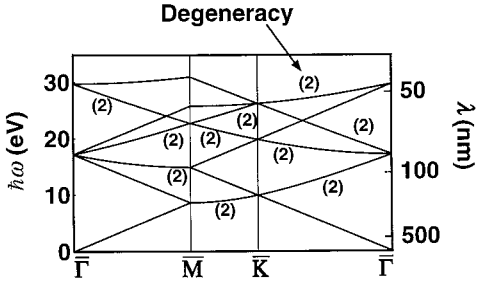

FIGURE 8 The first 10 photonic energy bands for the empty lattice model with parameters representing the cornea. The horizontal axis represents the triangular path around the irreducible segment of the Brillouin zone (Fig. 5), as in Figs. 6 and 7. The photon energy $\hbar\omega$ is given in electron volts and as the corresponding vacuum wavelength $\lambda = \omega/2\pi c$. The degeneracies of the bands are given in parentheses unless the bands are nondegenerate.

is not exceptionally large. The dielectric contrast is the ratio of the larger dielectric constant to the smaller, which is $\epsilon_f/\epsilon_b \approx 1.3$ for the cornea. In artificial dielectric structures, the dielectric can be made larger, and this exaggerates the changes from the empty lattice model. An example of the photonic band structure resulting from a larger dielectric contrast is shown in Fig. 9 for the same type of two-dimensional triangular lattice of rods as is used for the cornea lattice model. The contrast used in Fig. 9 is $\epsilon_b/\epsilon_f \approx 13$. Because the frequency is plotted in the dimensionless units $\omega a/2\pi c$, the bands depend only on the dielectric contrast and the filling fraction, which in Fig. 9 is given by $f = 0.8358$. (Recall that f is the fractional volume occupied by the rods, which here have the smaller dielectric constant.) This is the filling fraction and dielectric contrast that was found to be optimal for creating band gaps (Plihal and Maradudin, 1991; Maradudin and McGurn, 1993). Here the changes from the empty lattice band structure are quite pronounced, with considerably larger band gaps and band splittings. In fact, the splittings are so large that there appears to be a band gap for all $\vec{k}_{\|}$ values (Plihal and Maradudin, 1991; Maradudin and McGurn, 1993). An example of such a gap is the shaded frequency interval shown for each polarization in Fig. 9. Such a gap is of interest in artificial semiconductor structures because light of this frequency cannot propagate in any direction, so that light can be guided by a suitably designed structure.

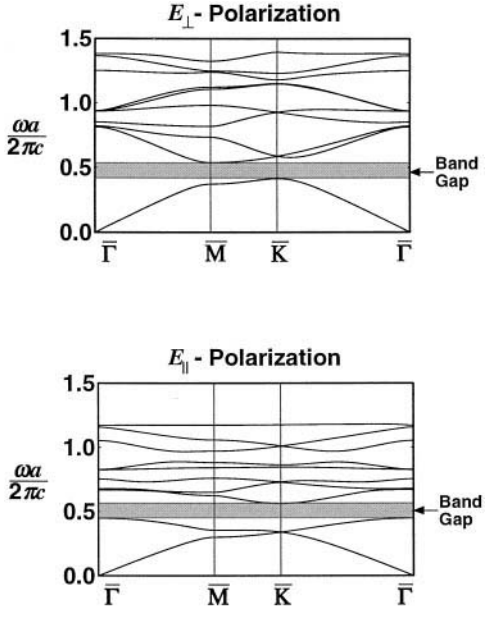

FIGURE 9 The first 10 photonic energy bands for the high contrast dielectric lattice of Maradudin and McGurn (1993). The horizontal axis represents the triangular path around the irreducible segment of the Brillouin zone (Fig. 5), as in Figs. 6–8. The shaded regions are believed to be two-dimensional band gaps extending throughout the Brillouin zone.

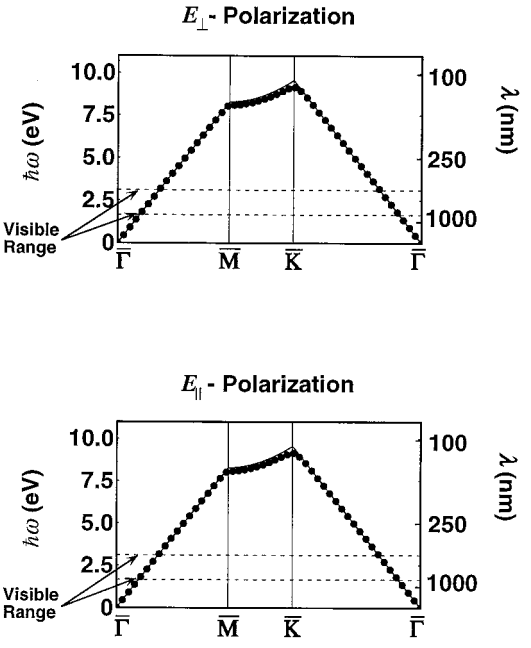

FIGURE 10 Effective medium approximation for the cornea lattice model. Only the lowest band is shown. The results of the full photonic band structure (Fig. 6) are shown as points, and the effective medium approximation is the solid curve. The effective medium approximation gives excellent agreement with the full photonic band structure computations over the visible region.

Effective medium approximation

Fig. 10 is a plot of the lowest band from Fig. 6, which shows the photonic band structure for the cornea model. Over the visible range, which is the range for which our dielectric constants are appropriate, the dispersion relation is practically linear along radial directions in $\vec{k}_{\|}$ space. That is, the dispersion relation over this region looks like a cone, as is true in a uniform medium. The dispersion relation can thus be written in the form of Eq. 7. However, the dielectric constant that must be used in that equation is neither that of the fibril nor that of the background, but an effective medium value ϵ_{eff} that lies between these two. We determine the value of this effective medium dielectric constant by fitting the cone-shaped linear dispersion of the empty lattice,

$$\omega = \frac{c}{\sqrt{\epsilon_{\text{eff}}}} k, \tag{34}$$

to the low-frequency region of the dispersion relation calculated from photonic band structure. The result of this fit is shown as the solid curves in Fig. 10, where it is compared with the calculated band structure as shown by the dots.

We find that this effective medium dielectric constant is different for the two polarizations and so is dependent on the orientation of the electric field, which is parallel to the fibrils in the $E_\|$ polarization case and perpendicular to the fibrils in the $E_\perp$ polarization case. This means that the dielectric properties of the medium are represented by a slightly anisotropic diagonal dielectric tensor. For the cornea model, the values for the $E_\perp$ and $E_\|$ polarizations are $\epsilon_{\text{eff}}^{\perp} = 1.930$ and $\epsilon_{\text{eff}}^{\|} = 1.945$, respectively.

We can use this effective medium approximation to investigate transmission through and reflection from the cornea in the visible range, because the effective medium dielectric constant gives a good description of the dispersion relation in this frequency range. Consider a slab of uniform material with parallel faces, so that the incident light from medium 1 strikes the slab of medium 2 and the transmitted light emerges into medium 3. The fraction of light reflected is (Reitz et al., 1993)

$$R = \frac{r_{12}^2 + r_{23}^2 + 2r_{12}r_{23}\cos\beta}{1 + r_{12}^2 r_{23}^2 + 2r_{12}r_{23}\cos\beta}, \tag{35}$$

where r_{ij} is the reflection amplitude on passing from medium i to medium j and β is a phase factor specifying interference between the two interfaces. For light at normal incidence the reflection amplitude is

$$r_{ij} = \frac{\sqrt{\epsilon_i} - \sqrt{\epsilon_j}}{\sqrt{\epsilon_i} + \sqrt{\epsilon_j}}, \tag{36}$$

and the phase factor is

$$\beta = 2\omega t_2 \sqrt{\epsilon_2}/c, \tag{37}$$

where ω is the angular frequency of the light, t_2 is the thickness of the slab of medium 2, and ϵ_2 is its dielectric constant. If medium 1 is air and medium 3 is water, the dielectric constants are $\epsilon_1 = 1$, $\epsilon_3 = 1.77$, and $\epsilon_2 = \epsilon_{\text{eff}}$.

We choose a dielectric constant ϵ_{eff} that is close to our two values for the different electric field orientations, $\epsilon_{\text{eff}} = 1.94 \cong \epsilon_{\text{eff}}^{\parallel} \cong \epsilon_{\text{eff}}^{\perp}$, and a thickness of 0.5 mm to plot in Fig. 11 the fraction $T = 1 - R$ of the light that is transmitted through the slab (*solid curve*). Also shown are the experimental data in Fig. 4 of Hart and Farrell (1969) for comparison. Because the light reflects back and forth between the two surfaces of the slab, the fraction transmitted oscillates as a function of the frequency of the incident light. This comes from the factor $\cos\beta$ in Eq. 35. The inset shows an enlargement of the oscillations, where the maximum amplitude of oscillations is ~1%. If we had made this calculation for a semi-infinite medium, i.e., with a single surface, the result would just be $T = 1 - r_{12}^2 \cong 0.98$, which is about the same as the maximum transmissivity in Fig. 11. In an actual sample of cornea, a slice of material would not have perfectly parallel surfaces, and, because of nonuniformity of the surface, the thickness would vary over the sample. For these reasons, in an actual measurement, these oscillations may not be apparent, and one might observe merely the average value of about $T \cong 0.97$. There might also be corrections for light striking at nonnormal incidence because of rough surfaces.

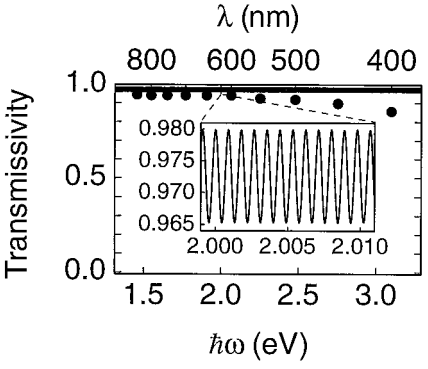

FIGURE 11 Effective medium calculation of the transmissivity of the cornea (*solid curve*) compared with experimental data (*solid dots*) from Hart and Farrell (1969) (Fig. 4). The fraction of light transmitted through a thin slab of dielectric material of thickness 0.5 mm is plotted; its dielectric constant is the effective medium $\epsilon_{\text{eff}} = 1.94$ found for the cornea. The transmitted light intensity appears as a thick line at ~97 ± 1% transmissivity because it is a rapidly oscillating function of the light frequency ω that is not resolved on the scale of this plot. These oscillations can be seen clearly in the expanded view shown in the inset.

The simplicity of this estimate illustrates the value of finding the effective medium parameters as we have done here. In contrast, Hart and Farrell presented an estimate of the light transmitted through the cornea using an approach that neglected the effects of multiple scattering and required the evaluations of a complicated formula (Hart and Farrell, 1969). Their evaluation of this formula used summations of large numbers of terms that nearly canceled each other, and calculations made in this way are subject to large round-off errors. The variations in these results with frequency may be due to such errors, because their calculations, like ours, did not include effects of absorption. This is one of the reasons we have emphasized that our calculations are only relevant to the cornea and sclera in the visible region. Nevertheless, their results give a transmissivity similar to ours and to some experimental data in the visible range. Experimental data do indicate that the transmissivity decreases substantially as the frequency approaches the ultraviolet, and this is likely due to large protein absorption bands in that region.

The effect of the anisotropy of the dielectric tensor is very minor here. It is of considerably more importance when both the dielectric contrast and filling fraction are high, as in the calculations of Maradudin and McGurn (1993). In those calculations, the dielectric contrast is $\epsilon_b/\epsilon_f \approx 13$ and the filling fraction is $f = 0.8358$, in comparison with $\epsilon_f/\epsilon_b \approx 1.3$ and $f = 0.23$ for the cornea. Our calculations of their lowest band for each of the $E_\perp$ and $E_\parallel$ polarizations are shown as dots in Fig. 12. The slopes of the linear dispersion relations at low frequencies are quite different for the $E_\perp$ and $E_\parallel$ polarizations. We determine the value of the effective medium dielectric constant for this system by fitting the cone-shaped linear dispersion relations of the empty lattice from Eq. 34 as we did for the cornea. This procedure gives effective dielectric constants $\epsilon_{\text{eff}}^{\perp}/\epsilon_f = 1.74$ and $\epsilon_{\text{eff}}^{\parallel}/\epsilon_f = 2.66$ for the $E_\perp$ and $E_\parallel$ polarizations, respectively. Therefore biological systems with higher dielectric contrast would have a larger anisotropy in the dielectric tensor.

CONCLUSIONS

The work presented here is believed to be the first application of the methods of photonic band structure to any

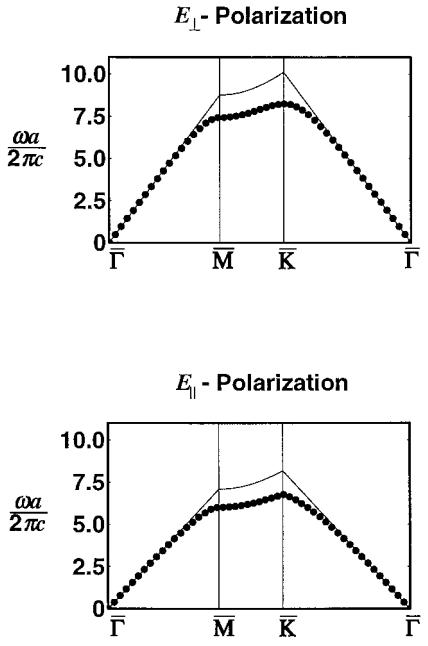

FIGURE 12 Effective medium approximation for the dielectric lattice of Maradudin and McGurn (1993). Only the lowest band is shown. The results of the full photonic band structure (Fig. 9) are shown as points, and the effective medium approximation is the solid curve. The effective medium approximation again gives good agreement with the full photonic band structure computations over the low-frequency region, with different effective medium dielectric constants for the two different polarizations.

biological system. Such calculations give the exact solution to Maxwell's equations for an ordered system. This restriction to an ordered system, however, requires that ordered models of the tissues be developed. We have done this for both the cornea and the sclera, and we find an intriguing difference between the two. In the cornea model, we find that visible light propagates as if it were in a uniform medium, although with an effective medium dielectric constant ϵ_{eff}, and we have shown how this effective dielectric constant can be determined. This implies that the cornea is transparent to visible light. In the sclera model, the bands in the visible region are noticeably distorted from what would occur in a uniform medium, and small band gaps occur in the visible. The distortions of these bands must certainly affect the transmission of light in the sclera and may be one of the factors leading to its opacity. We have calculated the transmissivity for the cornea model and have found that ~97% of the light would be transmitted. For the sclera, the calculations of transmitted light are more complex and will be a subject of future work.

Previous explanations of transparency versus opacity in the cornea hypothesized that if the wavelength of light is long compared with the fibril spacing, as it is the cornea, the material would be transparent, and if the vacuum wavelength is on the order of the fibril spacing, as in the sclera, it would be opaque (Benedek, 1971; Vaezy and Clark, 1991). Unfortunately, previous calculations neglected effects of multiple scattering, and some of the computations had inherent numerical difficulties (Hart and Farrell, 1969; Benedek, 1971; Vaezy and Clark, 1991), so that work was inconclusive. In contrast, computations of photonic band structure provide an essentially exact solution of Maxwell's equations. The price that must be paid for this is that an ordered model must be assumed. One conclusion that emerges from these solutions is that both the dielectric contrast and filling fraction, in addition to the ratio of vacuum wavelength to fibril spacing, are important in governing light propagation in a two-component tissue.

Although the cornea and sclera are not perfectly ordered systems, as was assumed for our models, the results nevertheless should give reasonable approximations of the way light propagates through these tissues. The cornea is actually fairly well ordered, while the sclera has a high degree of disorder. We expect the disorder to smear out the band structure to some extent, while leaving the main features. It is possible that the disorder, in conjunction with the band gaps, will be needed to give a complete picture of opacity in the sclera. In the general treatment of transparency and opacity in biological materials, it will be necessary to incorporate the effects of absorption. These are subjects that we hope to address in future work.

REFERENCES

Ameen, D. B. 1996. Theory of transparency of the cornea using photonic band structure. M.S. thesis, Virginia Commonwealth University.

Ameen, D. B., M. F. Bishop, and T. McMullen. 1996. Theory of transparency of the eye using photonic band structure. *Biophys. J.* 70:A431.

Benedek, G. B. 1971. Theory of transparency of the eye. *Appl. Optics. 3:459–473.*

Born, M., and K. Huang. 1968. Dynamical theory of crystal lattices. Oxford University Press, New York.

Brillouin, L. 1953. Wave Propagation in Periodic Structures: Electric Filters and Crystal Lattices. Dover, New York.

Cassagne, D., C. Jouanin, and D. Bertho. 1995. Photonic band gaps in a two-dimensional graphite structure. *Phys. Rev. B.* 52:R2217–R2220.

Doyle, B. B., E. G. Bendit, and E. R. Blout. 1975. Infrared spectroscopy of collagen and collagen-like polypeptides. *Biopolymers.* 14:937–957.

Economou, E. N., and A. Zdetsis. 1989. Classical wave propagation in periodic structures. *Phys. Rev. B.* 40:1334–1337.

Farrell, R. A., and R. W. Hart. 1969. On the theory of the spatial organization of macromolecules in connective tissue. *Bull. Math. Biophys.* 31:727–760.

Feng, Y., G. Melacini, and M. Goodman. 1997. Collagen-based structures containing the peptoid residue *N*-isobutylglycine (Nleu): synthesis and biophysical studies of Gly-Nleu-Pro sequences by circular dichroism and optical rotation. *Biochemistry.* 36:8716–8724.

Hart, R. W., and R. A. Farrell. 1969. Light scattering in the cornea. *Optical Soc. Am.* 59:766–774.

Ho, K. M., C. T. Chan, and C. M. Soukoulis. 1990. Existence of a photonic gap in periodic dielectric structures. *Phys. Rev. Lett.* 65:3152–3155.

Hopfield, J. J. 1966. Aspects of polaritons. *J. Phys. Soc. Jpn.* 21(Suppl.): 77–88.

Joannopoulos, J. D., R. D. Meade, and J. N. Winn. 1995. Photonic Crystals. Princeton University Press, Princeton, N.J.

John, S. 1987. Strong localization of photons in certain disordered dielectric superlattices. *Phys. Rev. Lett.* 58:2486–2489.

John, S. 1993. The localization of light. *In* Photonic Band Gaps and Localization. C. M. Soukoulis, editor. Plenum Press, New York. 1–22.

John, S., and R. Rangarajan. 1988. Optimal structures for classical wave localization: an alternative to the Ioffe-Regel criterion. *Phys. Rev. B.* 38:10101–10104.

Kronfeld, P. C. 1969. The gross anatomy and embryology of the eye. *In* The Eye, 2nd Ed. H. Davison, editor. Academic Press, New York. 1–66.

Leung, K. M., and Y. F. Liu. 1990a. Full vector wave calculation of photonic band structures in face-centered-cubic dielectric media. *Phys. Rev. Lett.* 65:2646–2649.

Leung, K. M., and Y. F. Liu. 1990b. Photon band structures: the plane-wave method. *Phys. Rev. B.* 41:10188–10190.

Maradudin, A. A., and A. R. McGurn. 1993. Photonic band structures of two-dimensional dielectric media. *In* Photonic Band Gaps and Localization. C. M. Soukoulis, editor. Plenum Press, New York. 247–268.

Maurice, D. M. 1957. The structure and transparency of the cornea. *J. Physiol. (Lond.).* 136:263–286.

Maurice, D. M. 1969. The Cornea and Sclera. *In* The Eye, 2nd Ed. H. Davison, editor. Academic Press, New York. 489–600.

Plihal, M., and A. A. Maradudin. 1991. Photonic band structure of two-dimensional systems: the triangular lattice. *Phys. Rev. B.* 44:8565–8571.

Reitz, J. R., F. J. Milford, and R. W. Christy. 1993. Foundations of Electromagnetic Theory. Addison-Wesley, Reading, MA.

Vaezy, S., and J. I. Clark. 1991. A quantitative analysis of transparency in the human sclera and cornea using Fourier methods. *J. Microsc.* 163: 85–94.

Yablonovitch, E. 1987. Inhibited spontaneous emission in solid-state physics and electronics. *Phys. Rev. Lett.* 58:2059–2062.

Yablonovitch, E., and T. J. Gmitter. 1989. Photonic band structure: the face-centered cubic case. *Phys. Rev. Lett.* 63:1950–1953.

Zhang, Z., and S. Satpathy. 1990. Electromagnetic wave propagation in periodic structures: Bloch wave solution of Maxwell's equations. *Phys. Rev. Lett.* 65:2650–2653.